Article

Immunity

Nephrocytes Remove Microbiota-Derived Peptidoglycan from Systemic Circulation to Maintain Immune Homeostasis

Graphical Abstract

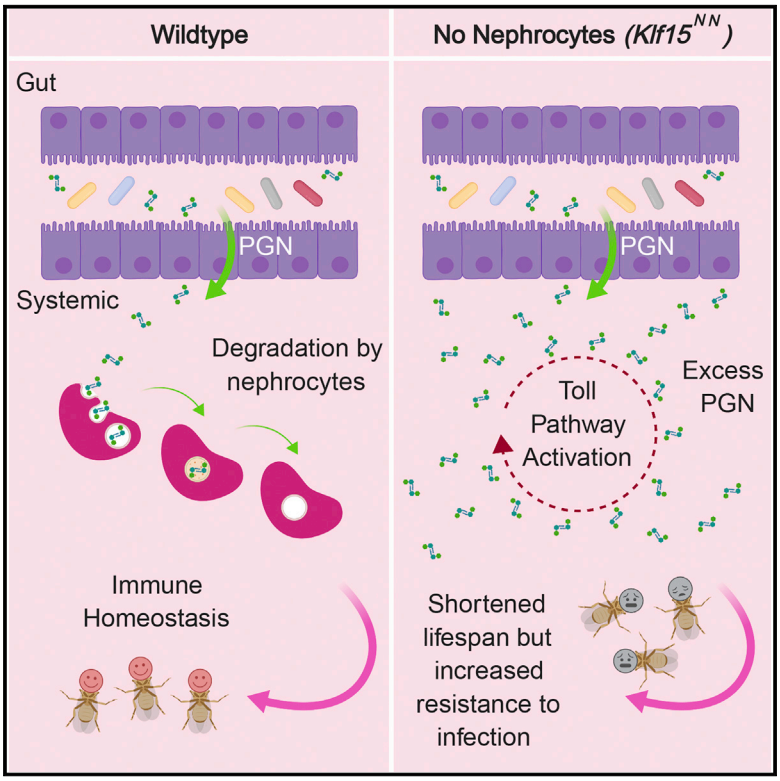

Authors

Katia Troha, Peter Nagy, Andrew Pivovar, Brian P. Lazzaro, Paul S. Hartley, Nicolas Buchon

Correspondence

nicolas.buchon@cornell.edu

In Brief

Troha et al. reveal that renal filtration of microbiota-derived peptidoglycan at steady state prevents aberrant immune activation, thus maintaining immune homeostasis in *Drosophila*. This function is likely conserved in mammals, with relevance to the chronic immune activation seen in settings of impaired blood filtration.

Highlights

- *Klf15*^{NN} flies display increased resistance to infection and a shorter lifespan
- *Klf15*^{NN} flies show systemic PGN accumulation and Toll pathway activation
- Germ-free conditions rescue the pathology of *Klf15*^{NN} flies
- Nephrocytes uptake microbiota-derived PGN and degrade it inside lysosomes

Troha et al., 2019, Immunity *51*, 625–637
October 15, 2019
https://doi.org/10.1016/j.immuni.2019.08.020

CellPress

Immunity
Article

Nephrocytes Remove Microbiota-Derived Peptidoglycan from Systemic Circulation to Maintain Immune Homeostasis

Katia Troha,[1] Peter Nagy,[1] Andrew Pivovar,[1] Brian P. Lazzaro,[1] Paul S. Hartley,[2] and Nicolas Buchon[1,3,*]
[1]Cornell Institute of Host-Microbe Interactions and Disease, Department of Entomology, Cornell University, Ithaca, NY, USA
[2]Department of Life and Environmental Science, University of Bournemouth, Talbot Campus, Poole, Dorset BH12 5BB, UK
[3]Lead Contact
*Correspondence: nicolas.buchon@cornell.edu
https://doi.org/10.1016/j.immuni.2019.08.020

SUMMARY

Preventing aberrant immune responses against the microbiota is essential for the health of the host. Microbiota-shed pathogen-associated molecular patterns translocate from the gut lumen into systemic circulation. Here, we examined the role of hemolymph (insect blood) filtration in regulating systemic responses to microbiota-derived peptidoglycan. *Drosophila* deficient for the transcription factor *Klf15* (*Klf15*^{NN}) are viable but lack nephrocytes—cells structurally and functionally homologous to the glomerular podocytes of the kidney. We found that *Klf15*^{NN} flies were more resistant to infection than wild-type (WT) counterparts but exhibited a shortened lifespan. This was associated with constitutive Toll pathway activation triggered by excess peptidoglycan circulating in *Klf15*^{NN} flies. In WT flies, peptidoglycan was removed from systemic circulation by nephrocytes through endocytosis and subsequent lysosomal degradation. Thus, renal filtration of microbiota-derived peptidoglycan maintains immune homeostasis in *Drosophila*, a function likely conserved in mammals and potentially relevant to the chronic immune activation seen in settings of impaired blood filtration.

INTRODUCTION

As the first line of defense against invading microorganisms, the innate immune system senses and responds to both pathogen-associated molecular patterns (PAMPs) and damage-associated molecular patterns (DAMPs) (Newton and Dixit, 2012). Peptidoglycan (PGN), a major constituent of the microbial cell wall, is an immune-stimulatory PAMP found in all bacteria. Following infection, detection of PAMPs in systemic circulation triggers a cascade of immune reactions that, if uncontrolled, can ultimately lead to sepsis (Cecconi et al., 2018). Even in the absence of infection, organisms are not a sterile environment—the animal gut and other mucosal tissues harbor numerous microbial species, which constitute the microbiota. A consequence of the presence of microbiota is the translocation of microbiota-shed PAMPs from the gut lumen into systemic circulation. This is a phenomenon that has been documented in a variety of organisms, including *Drosophila* and mammals (Capo et al., 2017; Clarke et al., 2010; Corbitt et al., 2013; Gendrin et al., 2009; Paredes et al., 2011; Zaidman-Rémy et al., 2006).

Drosophila is a powerful system to study innate immune responses to both pathogens and gut microbes (Buchon et al., 2014; Liu et al., 2017). To resist infection, *Drosophila* relies on both cellular and humoral innate immune responses. The cellular response consists of encapsulation and phagocytosis, while the humoral response involves the melanization cascade and the synthesis of antimicrobial peptides (AMPs) by the fat body, an organ analogous to the liver and adipose tissue of mammals. Production of AMPs is controlled by two principal signaling cascades: the Toll and Imd pathways. Both pathways are activated in response to PGN: Lys-type PGN from Gram-positive bacteria triggers the Toll pathway, while DAP-type PGN from Gram-negative bacteria and certain Gram-positive bacilli induces the Imd pathway (Buchon et al., 2014). In the fly, PGN is detected by peptidoglycan recognition proteins (PGRPs). PGRP-LC and PGRP-LE sense DAP-type PGN, and PGRP-SA recognizes Lys-type PGN (Kaneko et al., 2006; Michel et al., 2001). *Drosophila* possesses several immune mechanisms to both shape the microbiota and prevent excessive immune responses upon detection of microbial stimuli (Basbous et al., 2011; Cao et al., 2013; De Gregorio et al., 2002; Gordon et al., 2008; Levashina et al., 1999; Maillet et al., 2008; Scherfer et al., 2008; Thevenon et al., 2009). In the case of the Imd pathway, these mechanisms include negative regulators that avert excessive immune activation in response to the microbiota. For instance, the transcription factor Caudal suppresses Imd-dependent expression of AMPs in the gut, thereby shaping microbiota composition (Ryu et al., 2008). Another regulator, Pirk, sequesters PGRP-LC to prevent its exposure to microbiota-derived PGN and subsequent activation of the Imd pathway (Aggarwal et al., 2008; Kleino et al., 2008; Lhocine et al., 2008). Finally, secreted PGRPs with amidase activity scavenge and degrade immunostimulatory DAP-type PGN in order to block Imd activation (Paredes et al., 2011). A notable example of this is PGRP-LB, which is released into the hemolymph (extracellular fluid analogous to blood) to degrade translocated, microbiota-derived PGN, thus preventing systemic immune activation (Paredes et al., 2011; Zaidman-Rémy et al., 2006). Although the Toll

pathway also responds to the presence of PGN, little is known about the mechanisms that suppress Toll activation in response to microbiota and whether these have a role in the regulation of systemic responses.

The excretory system of *Drosophila* is composed of nephrocytes (which regulate hemolymph composition by filtration followed by filtrate endocytosis) and Malpighian tubules (which modify and secrete urine) (Denholm and Skaer, 2009; Hartley et al., 2016). *Drosophila* nephrocytes can be divided into two distinct groups: the garland cells, which appear as a necklace-like structure surrounding the esophagus, and the pericardial cells that form two rows of cells flanking the heart (Aggarwal and King, 1967; Crossley, 1972; Na and Cagan, 2013). In the adult stage, pericardial nephrocytes serve as the primary filtration units (Zhang et al., 2013). Hemolymph filtration occurs in a stepwise manner. First, hemolymph is filtered across the nephrocytes' negatively charged basement membrane and a specialized filter known as the nephrocyte diaphragm. The filtrate then enters the lacunae, also known as the labyrinthine channels, which extend several microns into the nephrocyte's cortical region (Kosaka and Ikeda, 1983). It is in these chambers where the filtrate is finally endocytosed by nephrocytes (Denholm and Skaer, 2009). Nephrocytes possess significant molecular, anatomical, and functional similarities to the glomerular podocyte, a cell type of the mammalian kidney important for the kidney's filtration function (Weavers et al., 2009; Zhuang et al., 2009). Both podocytes and nephrocytes possess a slit diaphragm and act as size- and charge-selective filters in the sequestration of materials from the blood and hemolymph (Reiser and Altintas, 2016; Weavers et al., 2009). The *Drosophila* ortholog of mammalian *Klf15*, a transcription factor required for podocyte differentiation (Mallipattu et al., 2012), is restricted to and essential for nephrocyte differentiation and function (Ivy et al., 2015). Flies that are mutant for *dKlf15* are viable but lack both garland and pericardial nephrocytes in the adult (Ivy et al., 2015). These flies thus enable study of the impact of hemolymph filtration in the maintenance of immune homeostasis.

Here, we found that flies devoid of nephrocytes ($Klf15^{NN}$ null allele), or with diminished nephrocyte function, were more resistant to a variety of microbial infections. $Klf15^{NN}$ flies exhibited improved survival upon infection but also a shorter lifespan stemming from abnormal Toll pathway activation. Aberrant Toll signaling in $Klf15^{NN}$ flies was dependent on the presence of Lys-type PGN microbiota. Microbiota-derived PGN accumulated in the hemolymph of these flies, triggering chronic stimulation of the Toll pathway. In wild-type (WT) flies, microbiota-derived Lys-type PGN found in systemic circulation was taken up by nephrocytes via endocytosis and degraded within lysosomes. Thus, renal filtration of microbiota-derived PGN maintains immune homeostasis in *Drosophila*, a function likely conserved in mammals.

RESULTS

$Klf15^{NN}$ Flies Are Less Susceptible to Microbial Infection

In order to evaluate the role of hemolymph filtration in immune function and homeostasis, we turned to flies that are mutant for the transcription factor *Klf15* ($Klf15^{NN}$ null allele), which lack nephrocytes. First, we confirmed that $Klf15^{NN}$ flies fail to develop nephrocytes (Figure 1A; Ivy et al., 2015). $Klf15^{NN}$ flies exhibited a significantly shorter basal lifespan compared to WT controls of the same genetic background (Figure 1B). Despite having a curtailed life expectancy, $Klf15^{NN}$ flies survived sterile wounding comparably to WT animals (Figures 1C–1G). To determine whether immune competence was affected by the loss of hemolymph filtration, we conducted survival assays with $Klf15^{NN}$ flies following systemic infection with the bacterial pathogens *Serratia marcescens* type strain, *Salmonella typhimurium*, *Listeria innocua*, *Enterococcus faecalis*, *Staphylococcus aureus*, and *Providencia rettgeri*. $Klf15^{NN}$ flies displayed significantly increased survival against five of these infections (Figures 1C–1G). The only exception was infection with *P. rettgeri*, to which the mutant proved more sensitive (Figure S1A). We did not observe a survival phenotype following challenge with two fungal agents, *Metarhizium anisopliae* and *Beauveria bassiana* (Figures S1B and S1C). Overall, these results suggest that $Klf15^{NN}$ flies are broadly protected against systemic infection by bacterial pathogens.

To verify that the enhanced survival observed in $Klf15^{NN}$ flies was a direct consequence of the loss of nephrocytes, we generated nephrocyte-deficient flies through complementary means. Using the nephrocyte-specific driver *Dot-Gal4*, we decreased *Klf15* expression by *in vivo* RNAi throughout development (*Dot-Gal4 > UAS-Klf15-IR*), which results in adult flies lacking nephrocytes (Ivy et al., 2015). Upon infection with *S. aureus* and *E. faecalis*, these flies displayed increased survival relative to the WT controls (Figures 1H and S1D). Next, we set out to determine whether the survival phenotype of $Klf15^{NN}$ flies resulted from loss of hemolymph filtration in the mutant or from a developmental defect associated with the loss of nephrocytes. To distinguish between the two possibilities, we took advantage of the fact that adult-specific loss of *Klf15* halts the endocytic function of mature nephrocytes (Ivy et al., 2015). We decreased *Klf15* expression by *in vivo* RNAi specifically during the adult stage using the conditional, nephrocyte- and heart-specific driver $Hand\text{-}Gal4^{ts}$ ($Hand\text{-}Gal4^{ts}$ > *UAS-Klf15-IR*) and infected these flies separately with *S. aureus* and *E. faecalis*. Diminishing the endocytic competence of adult nephrocytes by decreasing *Klf15* expression was sufficient to increase survival to infection with both bacteria (Figures 1I and S1E). Altogether, our results support the conclusion that loss of nephrocyte function generally increases survival against microbial infection.

$Klf15^{NN}$ Flies Are More Resistant to Infection, Independent of Phagocytosis and Melanization

Multicellular organisms employ two complementary strategies to combat infection: resistance, to eliminate microbes; and disease tolerance, to allow them to withstand the infection and/or its deleterious consequences (Ayres and Schneider, 2012). To determine whether the improved survival of $Klf15^{NN}$ flies was due to an increase in disease tolerance, we compared the bacterial load upon death (BLUD) of WT and $Klf15^{NN}$ flies following infection with *S. aureus* and *E. faecalis*. BLUD represents the maximal quantity of bacteria that an infected fly can sustain before it dies (Duneau et al., 2017) and is therefore one measure of disease tolerance. We found that control flies and $Klf15^{NN}$ flies die carrying similar numbers of each bacterium tested

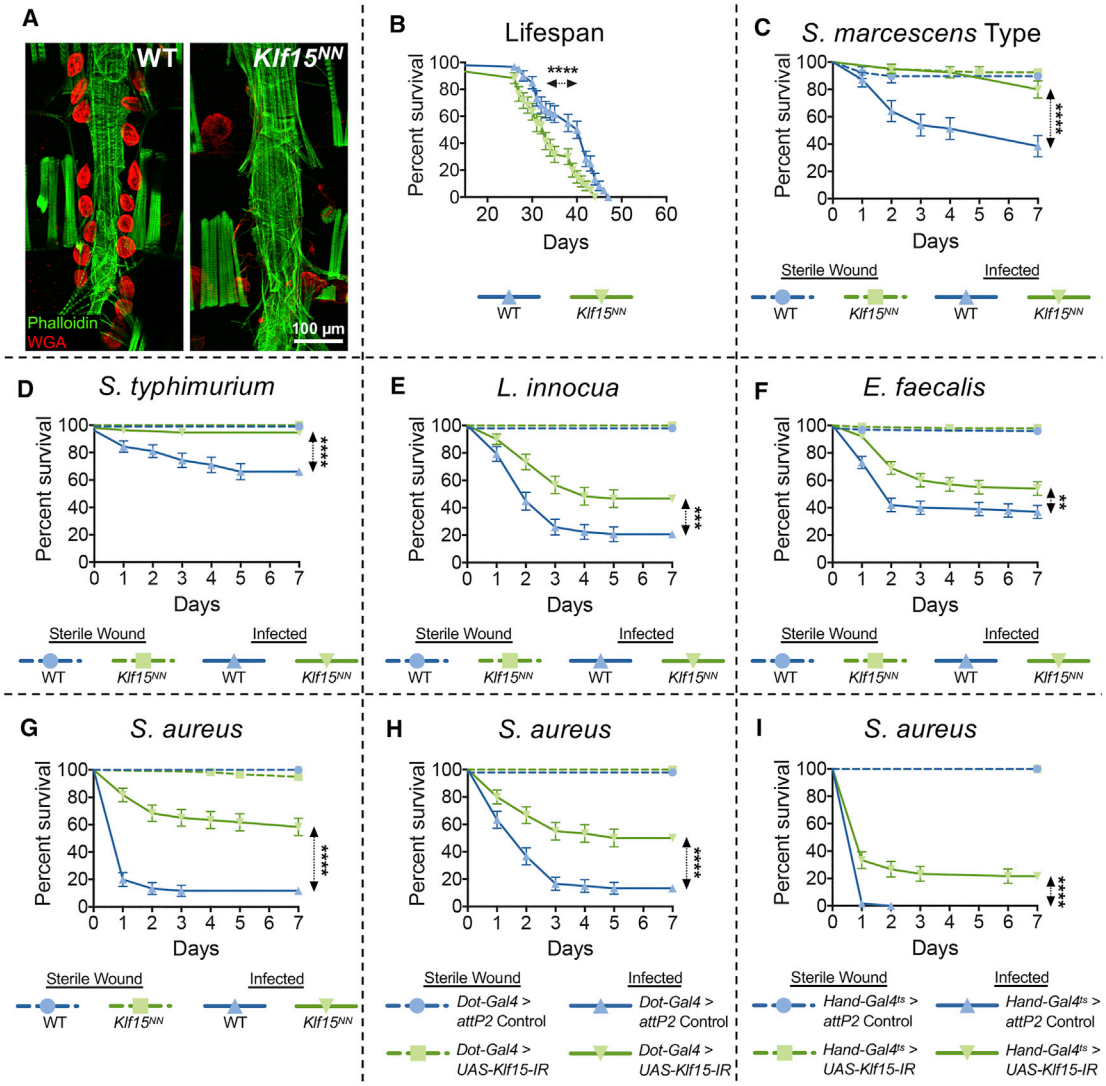

Figure 1. Loss of Nephrocyte Function Increases Survival against Infection

(A) Adult pericardial nephrocytes stained with WGA Alexa Fluor 594 conjugate (red). Phalloidin-FITC (green) marks the heart tube. Staining is shown for both wild-type (WT) and *Klf15*^{NN} flies.

(B) Lifespan curve comparing WT to *Klf15*^{NN} flies.

(C–G) Survival curves over 7 days following infection of WT and *Klf15*^{NN} flies with the bacterial pathogens: *S. marcescens* Type strain (C), *S. typhimurium* (D), *L. innocua* (E), *E. faecalis* (F), and *S. aureus* (G).

(H and I) Survival of flies expressing nephrocyte-specific RNAi against *Klf15* throughout development (*Dot-Gal4 > UAS-Klf15-IR*) (H) or only during the adult stage (*Hand-Gal4*^{ts} *> UAS-Klf15-IR)* (I) after infection with *S. aureus*.

The curves represent the average percent survival ± SE of three or more biological replicates. **p < 0.01 ***p < 0.001 ****p < 0.0001 in a Log-rank test.

(Figure S2A), indicating that this marker of disease tolerance is not altered in the mutant. Next, we tested whether the survival advantage of the mutant stemmed from improved resistance to infection. We monitored bacterial load during the course of *S. aureus*, *E. faecalis*, *S. marcescens*, *L. innocua*, and *S. typhimurium* infections (Figures 2A, 2B, and S2B–S2D). *Klf15*^{NN} flies carried significantly lower bacterial burdens than WT flies as soon as 3 h post-infection with *S. aureus*, 4.5 h after challenge with *E. faecalis*, and 6 h post-inoculation with *S. marcescens*, *L. innocua*, and *S. typhimurium*, demonstrating that flies without nephrocytes are more resistant to pathogens in the early stages of infection.

Drosophila relies primarily on three effector mechanisms to control bacterial growth: phagocytosis, melanization, and the production of AMPs. First, we evaluated a role for phagocytosis in the resistance phenotype of *Klf15*^{NN} flies. We injected nephrocyte-deficient and WT flies with pH-sensitive pHrodo bacteria, which become fluorescent only after being engulfed into a fully mature, acidified phagosome (Guillou et al., 2016). After quantification, we observed close to 50% less fluorescence in *Klf15*^{NN} flies relative to controls (Figure S2E). Moreover, injection of flies with latex beads prior to systemic infection with both *S. aureus* and *E. faecalis*, a treatment that blocks phagocytosis (Elrod-Erickson et al., 2000), did not alter

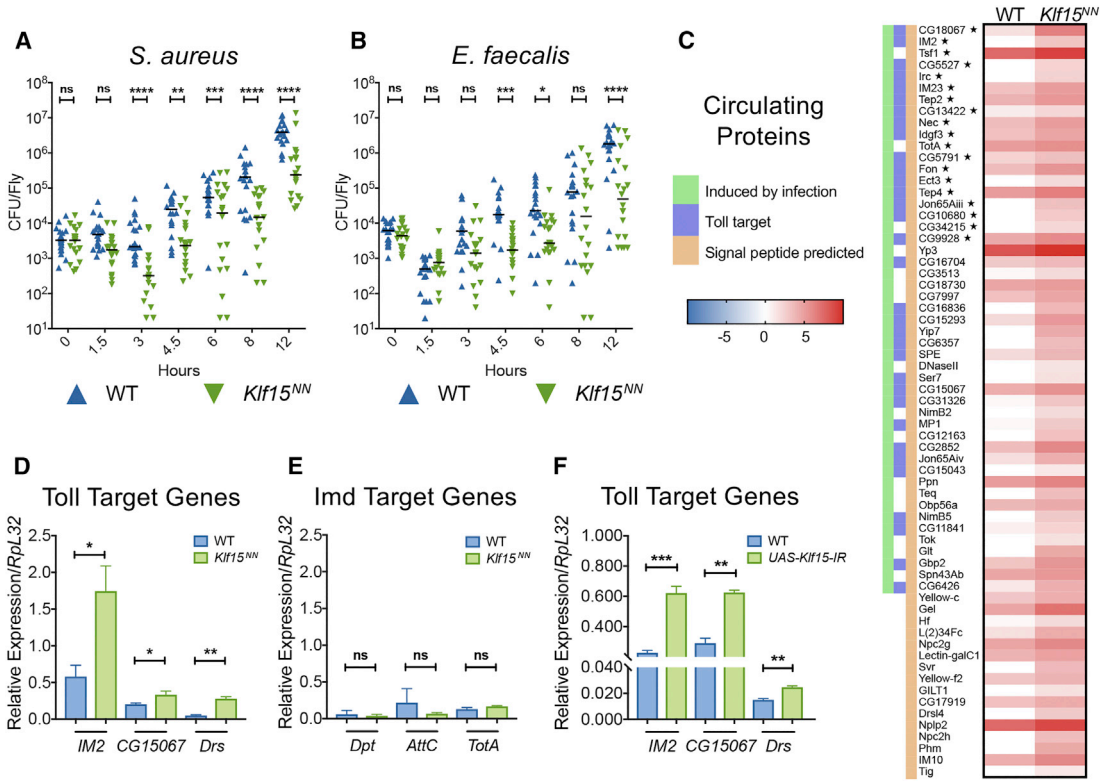

Figure 2. The Toll Pathway Is Activated in *Klf15*^{NN} Flies

(A and B) Bacterial load time course of control and *Klf15*^{NN} flies following infection with *S. aureus* (A) and *E. faecalis* (B). Three repeats are graphed together with each symbol representing an individual fly's number of colony forming units (CFU). Horizontal lines represent median values for each time point. Data were normalized and then analyzed using a two-way ANOVA followed by Sidak's post-test for specific comparisons (*p < 0.05 **p < 0.01 ***p < 0.001 ****p < 0.0001).

(C) Heatmap showing a list of circulating proteins enriched (≥ 1.5-fold) in the hemolymph (insect blood) of *Klf15*^{NN} flies over that of WT or only present in *Klf15*^{NN} flies but not WT. A color scale on the left side of the heatmap denotes whether the gene that encodes each protein is transcriptionally induced by infection (green), a target of the Toll pathway (blue), or predicted to possess a signal peptide (orange). Core genes are highlighted with a ★ symbol (Troha et al., 2018).

(D and E) Whole-fly qRT-PCR of Toll target genes *IM2*, *CG15067*, and *Drs* (D) and Imd target genes *Dpt*, *AttC*, and *TotA* (E) using unchallenged WT and *Klf15*^{NN} samples.

(F) Quantification of Toll target genes *IM2*, *CG15067*, and *Drs* via qRT-PCR in flies expressing RNAi against *Klf15* only during the adult stage (*Hand-Gal4*^{ts} > *UAS-Klf15-IR*). Mean values of three or more repeats are presented ± SE. *p < 0.05 **p < 0.01 ***p < 0.001 in a Student's t test.

the survival phenotype of *Klf15*^{NN} flies (Figures S2F and S2G). These results demonstrate that phagocytic activity does not contribute meaningfully to the increased resistance of *Klf15*^{NN} flies. Assessment of phenoloxidase (PO) activity, the terminal enzymatic step driving melanization, revealed that while *Klf15*^{NN} flies had significantly higher PO activity in basal conditions, they also displayed significantly lower PO activity relative to controls 3 h post infection with *S. aureus* and *E. faecalis* (Figure S2H). To clarify whether melanization played any role in the survival phenotype of *Klf15*^{NN} flies, we generated a mutant deficient for both *Klf15* and key genes required for the melanization response (*PPO1*$^{\Delta}$, *2*$^{\Delta}$,*3*^{1}) (Binggeli et al., 2014; Dudzic et al., 2015). Upon infection with *S. aureus*, the quadruple mutant (*Klf15*^{NN}; *PPO1*$^{\Delta}$, *2*$^{\Delta}$,*3*^{1}) exhibited improved survival relative to the triple mutant (*PPO1*$^{\Delta}$, *2*$^{\Delta}$,*3*^{1}) (Figure S2I), suggesting that melanization is not required for the protection observed in nephrocyte-deficient flies. In sum, our data indicate that loss of nephrocytes confers increased resistance to hosts independent of phagocytosis and melanization.

The Toll Pathway Is Constitutively Active in *Klf15*^{NN} Flies

Nephrocytes are major regulators of hemolymph content via filtration followed by filtrate endocytosis (Hartley et al., 2016; Soukup et al., 2009). Therefore, we considered whether changes in circulating proteins in the mutant could account for the increased resistance observed in *Klf15*^{NN} flies. Previously, we performed a proteomic analysis of hemolymph composition in both WT and *Klf15*^{NN} unchallenged flies (Hartley et al., 2016). An in-depth analysis of this dataset revealed that among 130 proteins enriched (≥ 1.5-fold) or detected only in the hemolymph of nephrocyte-deficient mutants, 65 proteins were annotated as having an immune-related function (Figure 2C). All 65 proteins were predicted to have a signal sequence (SignalP 4.1), which is expected for secreted hemolymph proteins. Of these 65 proteins, 19 were encoded by core genes of the *Drosophila* immune response (i.e., genes with increased transcription in response to most bacterial infections [Troha et al., 2018]), 30 were the products of genes that are induced only by a subset of microbial infections, and 16 were coded by genes that, while not regulated in response to infection themselves,

have been ascribed an immune function. We also noted that a majority (33 of 65) of these proteins are known targets of the Toll pathway (e.g., the antimicrobial peptide genes *IM2*, *IM23*, and *CG15067*). Thus, the hemolymph of *Klf15*^{NN} flies is enriched in proteins of immune function primarily encoded by target genes of the Toll pathway, suggesting that changes in Toll pathway activity may explain the increase in resistance to pathogens observed in *Klf15*^{NN} flies.

We developed two competing hypotheses to explain the accumulation of Toll pathway targets in the hemolymph of *Klf15*^{NN} flies. The first hypothesis posited that because nephrocytes are critical regulators of protein turnover in the hemolymph, the rise in immune effectors could be the result of a decrease in protein turnover in these flies. Alternatively, the accumulation of immune gene products could be due to aberrant activation of the Toll and/or Imd pathways in nephrocyte-deficient flies. In agreement with the latter hypothesis, our proteomic analysis also identified proteins that were depleted ($\geq$ 1.5-fold) in the hemolymph of *Klf15*^{NN} flies relative to controls (Figure S2J). Six of these proteins are encoded by genes that typically show decreased transcription in response to bacterial infection in a Toll-dependent manner (e.g., *Lsp1*β and *CG2233*) (Troha et al., 2018), arguing that changes in hemolymph protein content are due to Toll pathway activation rather than protein turnover. To test this idea directly, we surveyed the activation of the Toll and Imd pathways by measuring the mRNA expression of 5 Toll target genes and 4 Imd target genes in WT and *Klf15*^{NN} flies under basal conditions. qRT-PCR data from whole fly showed that the mRNA expression of all 5 Toll target genes—*IM2*, *CG15067*, *Drs*, *CG18067*, and *CG15293*—was significantly increased in *Klf15*^{NN} flies compared to controls (Figures 2D and S2K). In contrast, we did not find any appreciable differences in gene expression between WT and *Klf15*^{NN} flies for the Imd target genes *Dpt*, *AttC*, and *TotA*; the exception was *AttD*, for which the mutant had significantly lower mRNA expression relative to WT (Figures 2E and S2K). These data indicate that the Toll pathway, but not the Imd pathway, is constitutively activated in *Klf15*^{NN} flies in unchallenged conditions. In agreement with these data, we also detected abnormal Toll activation in flies in which *Klf15* expression was decreased by *in vivo* RNAi, specifically during the adult stage (*Hand-Gal4*^{ts} > *UAS-Klf15-IR*), demonstrating that the loss of nephrocyte scavenging function is solely responsible for Toll activation in these flies (Figure 2F). In contrast to our results in unchallenged conditions, infection of *Klf15*^{NN} flies with either *S. aureus* or *E. faecalis* revealed no significant differences between WT and mutant in terms of Toll or Imd target gene expression at any of the time points surveyed (3, 8, and 12 h post challenge) (Figures S2L and S2M). In conclusion, our data establish that *Klf15*^{NN} flies present elevated basal mRNA expression of Toll target genes in conjunction with increased immune resistance to pathogens.

Increased Pathogen Resistance in *Klf15*^{NN} Flies Is Contingent on Higher Baseline Toll Activity

Next, we asked whether Toll pathway activity could be responsible for the increased resistance observed in *Klf15*^{NN} flies. We began by verifying that the increase in baseline Toll target gene expression was dependent on the Toll pathway itself. qRT-PCR of the Toll target genes *IM2* (Figure 3A), *CG15067*, and *Drs* (Figures S3A and S3B) showed that a null mutation in the gene coding for the Toll cytokine Spz completely abolished the increase in Toll target gene expression found in *Klf15*^{NN} flies (*Klf15*^{NN}; *spz*^{rm7} double mutants). This was also true for a null mutation in the gene coding for SPE (*Klf15*^{NN}; *SPE*^{SK6}), a key enzyme involved in the maturation of Spz and subsequent activation of the Toll pathway (Figures S3C–S3E), demonstrating that the increase in Toll target gene expression in *Klf15*^{NN} flies is due to elevated Toll pathway activity. Notably, suppression of the Toll pathway by either *spz*^{rm7} or *SPE*^{SK6} completely abrogated the survival advantage of *Klf15*^{NN} flies against pathogenic infection (Figures 3B, 3C, S3F, and S3G). These results indicate that a surge in Toll pathway signaling is directly accountable for the augmented resistance of *Klf15*^{NN} flies to infection.

The Toll pathway can be induced by endogenous DAMPs, which trigger the maturation of the circulating serine protease Persephone (Psh), or by the recognition of PAMPs, leading to the activation of the serine protease ModSP (Buchon et al., 2009; Gottar et al., 2006; Ming et al., 2014). Consequently, we set out to investigate whether aberrant Toll signaling in *Klf15*^{NN} flies was dependent on the detection of DAMPs or PAMPs by the host. While a null allele of *psh* was unable to rescue the elevated basal expression of the Toll target genes *IM2* (Figure 3D), *CG15067*, and *Drs* (Figures S3H and S3I) in *Klf15*^{NN} flies (*Klf15*^{NN}, *psh*^{1}), a null mutation in *modSP* fully reverted this increase (*Klf15*^{NN}; *modSP*^{1}) (Figures 3G, S3J, and S3K). Accordingly, while the improved survival phenotype of *Klf15*^{NN} flies was still present in *Klf15*^{NN}, *psh*^{1} flies (Figures 3E and 3F), *Klf15*^{NN}; *modSP*^{1} flies no longer exhibited it (Figures 3H and 3I). Thus, our data support the conclusion that elevated Toll signaling in response to PAMPs is responsible for the *Klf15*^{NN} phenotype.

ModSP activity, and therefore Toll pathway signaling, can be induced by the binding of pattern recognition receptors (PRRs) to two types of PAMPs: β-(1,3)-glucan derived from the fungal cell wall is recognized by GNBP3 (Gottar et al., 2006), while bacterial PGN is detected by PGRP-SA (Michel et al., 2001). Thus, we moved to resolve whether the increase in Toll pathway activity observed in *Klf15*^{NN} flies was due to sensing of PGN by PGRP-SA or β-(1,3)-glucan by GNBP3. qRT-PCR of the Toll target genes *IM2*, *CG15067*, and *Drs* demonstrated that the increase in basal Toll pathway signaling present in *Klf15*^{NN} flies was downstream of PGRP-SA (*Klf15*^{NN} , *PGRP-SA*^{seml}) (Figures 3J, S3L, and S3M) but not GNBP3 (*Klf15*^{NN}; *GNBP3*^{Hades}) (Figures S3N–S3P). The enhanced survival phenotype of *Klf15*^{NN} flies was also lost in the double mutant *Klf15*^{NN} , *PGRP-SA*^{seml} (Figures 3K and 3L), but not in the double mutant *Klf15*^{NN}; *GNBP3*^{Hades} (Figures S3Q and S3R), indicating that the surge in Toll signaling observed in nephrocyte-deficient flies is likely downstream of PGN recognition. Finally, bacterial load data from the double mutants *Klf15*^{NN}; *modSP*^{1} and *Klf15*^{NN} , *PGRP-SA*^{seml} infected with *S. aureus* or *E. faecalis* showed that in absence of a functional Toll pathway, *Klf15*^{NN} flies no longer display reduced pathogen load compared to WT (Figures S3S and S3T), confirming that the increase in resistance observed in *Klf15*^{NN} flies is dependent on the Toll pathway.

Microbiota-Derived PAMPs Trigger Aberrant Toll Pathway Activation in *Klf15*^{NN} Flies

Gut microbes are a source of PAMPs, such as PGN, and therefore can act as elicitors of the immune system (Clarke et al.,

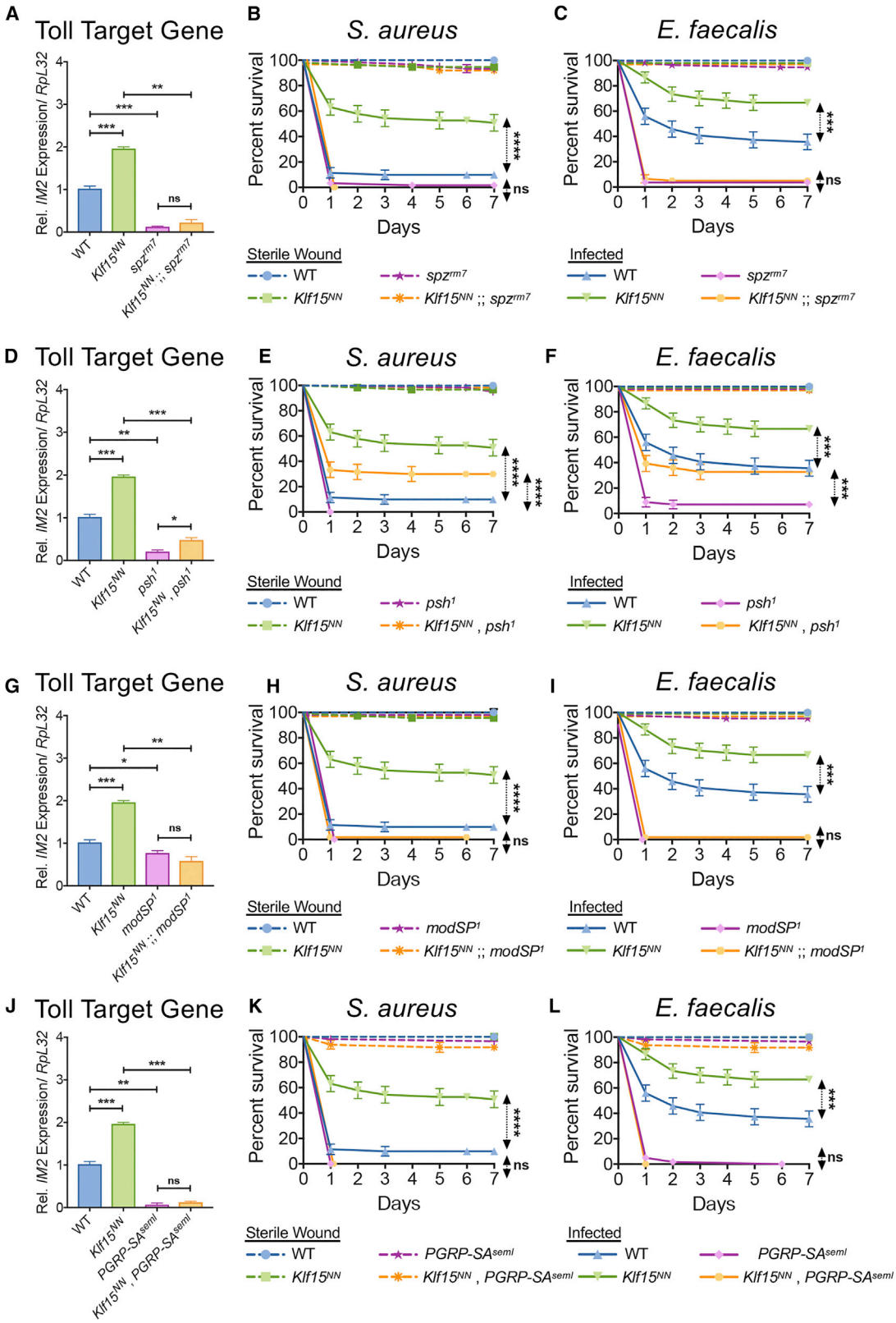

Figure 3. Increased Resistance to Infection in *Klf15*^{NN} Flies Is PGRP-SA-Dependent

(A–C) Comparison of *Klf15*^{NN}; *spz*^{rm7} double mutants to WT, *Klf15*^{NN} , and *spz*^{rm7} single mutants in experiments measuring *IM2* (Toll target) gene expression via qRT-PCR (A), survival against *S. aureus* (B), and survival against *E. faecalis* (C).

(legend continued on next page)

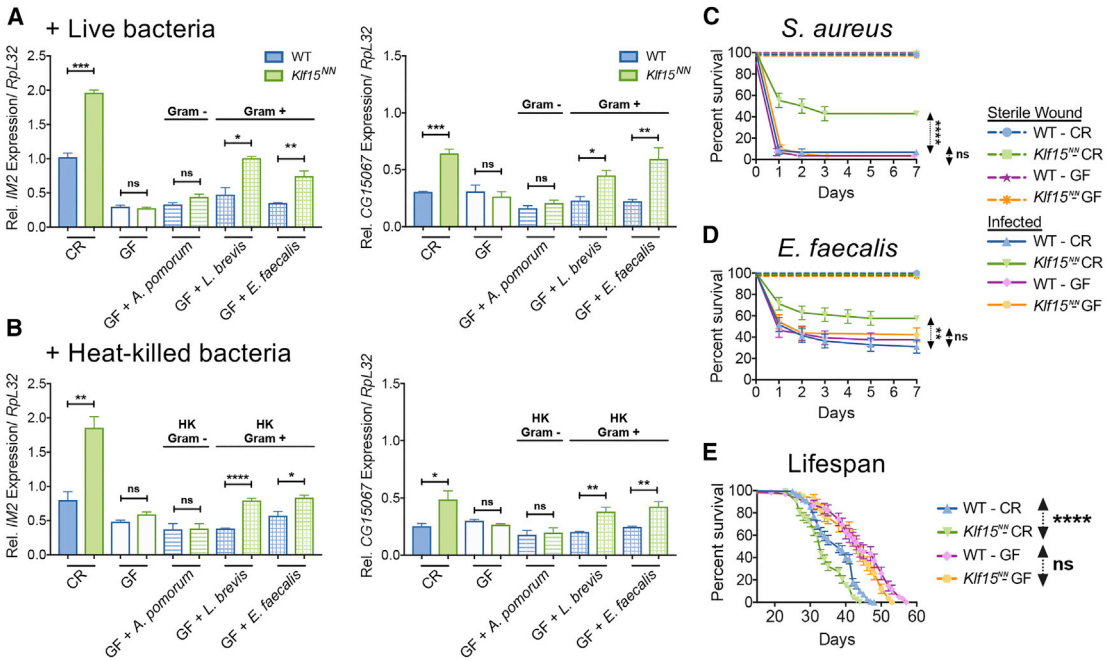

Figure 4. Nephrocytes Prevent Excessive Immune Activation Against Gram-Positive Microbiota

(A) Quantification of mRNA transcripts in conventional (CR), germ-free (GF), and germ-free flies recolonized with either live *A. pomorum* (Gram-negative), live *L. brevis* (Gram-positive), or live *E. faecalis* (Gram-positive). qRT-PCR measurements of Toll target genes *IM2* and *CG15067* are shown.

(B) Quantification of mRNA transcripts in CR, GF, and germ-free flies fed either heat-killed *A. pomorum* (Gram-negative), heat-killed *L. brevis* (Gram-positive), or heat-killed *E. faecalis* (Gram-positive). qRT-PCR measurements of Toll target genes *IM2* and *CG15067* are presented.

For qRT-PCR experiments, mean values of three or more repeats are given ± SE. *p < 0.05 **p < 0.01 ***p < 0.001 ****p < 0.0001 in a Student's t test.

(C and D) Survival curve over 7 days following infection of WT and *Klf15*^{NN} flies with *S. aureus* (C) and *E. faecalis* (D) in both CR and GF conditions.

(E) Lifespan curve comparing WT to *Klf15*^{NN} flies in both CR and GF conditions.

Survival curves give the average percent survival ± SE of three biological replicates (**p < 0.01 ****p < 0.0001 in a Log-rank test).

2010; Kaneko et al., 2004). In *Drosophila*, multiple mechanisms are in place to prevent undue activation of the Imd pathway in response to microbiota. These include the expression of a plethora of negative regulators (e.g., Caudal and Pirk) and enzymes that degrade DAP-type PGN (e.g., PGRP-LB and PGRP-SC). However, no similar mechanism has been described for the Toll pathway despite the fact that it also senses PGN (Lys-type) (Bischoff et al., 2004; Park et al., 2007). Because the increase in Toll pathway activity in *Klf15*^{NN} flies depends on PGRP-SA, we hypothesized that the phenotype could stem from an errant immune response against the microbiota. To test this idea, we used qRT-PCR to measure the mRNA expression of the Toll target genes *IM2*, *CG15067* (Figure 4A), and *Drs* (Figure S4A) in WT and *Klf15*^{NN} flies raised in both conventionally reared (CR) and germ-free (GF) conditions. We found that the increase in Toll signaling in *Klf15*^{NN} flies was fully dependent on the presence of microbiota, as GF WT and GF *Klf15*^{NN} flies displayed similar mRNA expression for all measured Toll target genes. Since *Klf15*^{NN} flies did not have a higher microbiota load or show any alteration in gut-barrier integrity—as determined by the SMURF assay and measurements of both circulating bacteria in the hemolymph and whole fly microbiota (Figures S4B–S4D)—our results indicate that *Klf15*^{NN} flies display aberrant Toll pathway activation in response to microbiota.

Because the increase in Toll pathway activity found in nephrocyte-deficient flies is both downstream of PGRP-SA and microbiota-dependent, we postulated that this phenotype could arise from an abnormal response to microbiota-derived PAMPs. In agreement with this hypothesis, mono-colonization of GF *Klf15*^{NN} flies with the Gram-positive, Lys-type PGN-carrying microbes *E. faecalis* and *Lactobacillus brevis* (*L. brevis*, like many other *Lactobacilli* spp., carries Lys-Asp-type PGN as previously described [Salvetti et al., 2012; Schleifer and Kandler, 1972]) triggered aberrant Toll pathway activity, while recolonization with the Gram-negative, DAP-type PGN-containing *Acetobacter pomorum* did not (Figures 4A and S4A). Of note, *E. faecalis*,

(D–F) Comparison of *Klf15*^{NN}, *psh*^{1} double mutants to WT, *Klf15*^{NN} , and *psh*^{1} single mutants in experiments measuring *IM2* gene expression via qRT-PCR (D), survival against *S. aureus* (E), and survival against *E. faecalis* (F).

(G–I) Comparison of *Klf15*^{NN}; *modSP*^{1} double mutants to WT, *Klf15*^{NN} , and *modSP*^{1} single mutants in experiments measuring *IM2* gene expression via qRT-PCR (G), survival against *S. aureus* (H), and survival against *E. faecalis* (I).

(J–L) Comparison of *Klf15*^{NN} , *PGRP-SA*^{seml} double mutants to WT, *Klf15*^{NN} , and *PGRP-SA*^{seml} single mutants in experiments measuring *IM2* gene expression via qRT-PCR (J), survival against *S. aureus* (K), and survival against *E. faecalis* (L).

For qRT-PCR experiments, mean values of three or more repeats are presented ± SE (*p < 0.05 **p < 0.01 ***p < 0.001 in a Student's t test). Survival curves show the average percent survival ± SE of three biological replicates (***p < 0.001 ****p < 0.0001 in a Log-rank test).

A. pomorum, and *L. brevis* are normal constituents of the *Drosophila* gut microbiota (Broderick et al., 2014). This result suggested that the microbiota could act to elevate Toll pathway signaling in nephrocyte-deficient flies by providing a source of Lys-type PGN, thus stimulating PGRP-SA in the absence of infection. Additional experiments confirmed that gut microbiota-derived PAMPs were sufficient to trigger the Toll pathway in GF $Klf15^{NN}$ flies. Feeding GF $Klf15^{NN}$ hosts with heat-killed *L. brevis* or *E. faecalis*, but not *A. pomorum*, was enough to elicit abnormal Toll pathway activity as measured by *IM2*, *CG15067*, and *Drs* expression (Figures 4B and S4E). Altogether, these results established that in $Klf15^{NN}$ flies, gut-microbiota-derived Lys-type PGN induces an errant, Toll pathway-mediated immune response.

Next, we explored whether this abnormal response to the microbiota could be responsible for the increase in resistance to infection observed in $Klf15^{NN}$ flies. Unlike flies raised in CR conditions, GF $Klf15^{NN}$ flies infected with the bacterial pathogens *S. aureus* and *E. faecalis* did not exhibit increased survival to infection relative to GF WT controls (Figures 4C and 4D). These results suggest that microbiota-derived Lys-type PGN primes the Toll pathway in $Klf15^{NN}$ flies, leading to enhanced resistance. Chronic immune activation is costly and harmful to hosts (Charroux et al., 2018; Guo et al., 2014; Paredes et al., 2011). As we noted that flies devoid of nephrocytes had a shorter lifespan (Figure 1B), we asked whether this could also be due to chronic immune activation in response to the microbiota. $Klf15^{NN}$ flies reared in GF conditions significantly outlived their CR counterparts, and no difference in lifespan was found between $Klf15^{NN}$ and WT flies raised in GF conditions (Figure 4E). Our results demonstrate that nephrocytes are part of a program that prevents microbiota-dependent Toll pathway activation, thus avoiding its deleterious effect on lifespan.

Nephrocytes Endocytose PGN from the Hemolymph to Avert Excessive Immune Activation in Response to Microbiota

We find that the Toll pathway is significantly activated in response to microbiota-derived PAMPs in the absence of nephrocytes. This could be the result of either the presence of elevated amounts of microbiota-shed PGN in the hemolymph (as microbiota-shed PAMPs are commonly translocated from the gut lumen into systemic circulation) or the hyper-reactivity of these flies to PAMPs. SPE, a signaling component of the Toll pathway, accumulates in the hemolymph of $Klf15^{NN}$ flies (Figure 2C) despite its mRNA not being transcriptionally increased (Figure S4I). Overexpression of SPE is also sufficient to trigger Toll pathway activation (Jang et al., 2006). Consequently, we hypothesized that accretion of SPE could result in an aberrant response to the microbiota in $Klf15^{NN}$ flies. While overexpression of SPE alone resulted in increased expression of three target genes of the Toll pathway, *IM2*, *CG15067*, and *Drs* (Figures S4F–S4H), the mRNA expression of these genes was identical between CR and GF conditions, suggesting that this effect was not dependent on the presence of microbiota. It is therefore unlikely that the microbiota-dependent induction of Toll in $Klf15^{NN}$ flies is due to SPE accumulation. In light of this result, we moved on to the next hypothesis. As nephrocytes regulate hemolymph composition by filtration followed by filtrate endocytosis, we reasoned that in the absence of nephrocytes, microbiota-derived Lys-type PGN could accumulate in the hemolymph. We therefore measured the amount of PGN circulating in the hemolymph of WT and $Klf15^{NN}$ flies in both CR and GF conditions. Using a colorimetric assay (SLP), we detected three times more circulating PGN in $Klf15^{NN}$ flies than in WT controls under CR conditions, with no difference found between the two genotypes under GF conditions (Figure 5A). These data establish that nephrocytes participate in the removal of microbiota-shed PGN from systemic circulation.

Subsequently, we focused on determining which mechanisms underlie nephrocyte-mediated PGN removal from hemolymph. Nephrocytes are filtration devices. Their surface is covered by extensive membrane invaginations, which are sealed at the top by slit diaphragms. These chambers, known as lacunae or labyrinthine channels, are where most of their endocytic activity takes place. Once endocytosed, internalized cargo is either trafficked to lysosomes for degradation, metabolized and released back into circulation, or stored in vacuoles for the lifespan of the fly (Denholm and Skaer, 2009; Psathaki et al., 2018). To assess whether nephrocytes internalize circulating PGN, we immunostained nephrocytes with an anti-PGN antibody (raised against PGN from a Gram-positive Streptococcus sp.). Confocal sectioning of nephrocytes revealed a strong punctate signal pattern, indicating that nephrocytes do indeed internalize PGN (Figure 5B, specifically 5B1). PGN staining disappeared in flies reared in GF conditions, suggesting that nephrocytes take up microbiota-derived PGN in order to remove it from the hemolymph (Figure 5B2, see Figure S5A for quantification). Immunostaining against PGN in nephrocytes expressing either a reporter for the early endosomal marker Rab5 (*Hand-Gal4^{ts} > UAS-Rab5-YFP*) or a reporter for the late endosomal marker Rab7 (*Hand-Gal4^{ts} > UAS-Rab7-YFP*) showed co-localization of PGN with both markers (Figure 5C, see Figure S5B for Pearson correlation coefficients). We also detected co-localization of PGN with the lysosomal markers cathepsin L and Lamp1 (Lysosomal associated membrane protein 1, Figures 5C, S5B, and S5C), implying that PGN is internalized by endocytosis and routed to the lysosomal compartment.

We then moved to evaluate the role of endocytosis in the uptake of PGN by nephrocytes. The dynamin Shibire is involved in the early steps of endocytosis. Blocking Shibire triggers elongation of the lacunae (also referred to as labyrinthine channels) within nephrocytes (Figure 5D, Duf labels the lacunae) (Kosaka and Ikeda, 1983; Psathaki et al., 2018). Because the filtration and endocytic functions of nephrocytes are separate, blocking endocytosis—but not filtration via expression of the thermosensitive *shibire^{ts1}* allele results in the accumulation of filtrate in the lacunae, a phenomenon previously observed with the circulating serpin Necrotic (Soukup et al., 2009). When we blocked the endocytic pathway using this same allele (*Hand-Gal4^{ts} > UAS-shi^{ts1}*), we observed the accumulation of PGN in the lacunae of nephrocytes (Figures 5B3, 5D, S5D1, and S5E), signifying that nephrocytes endocytose PGN by a Shibire-dependent mechanism. In addition, nephrocyte-specific expression of a dominant negative form of Rab5 (*Hand-Gal4^{ts} > UAS-Rab5^{DN}*, Rab5 is a key regulator of early endosomal trafficking) and Rab7 (*Hand-Gal4^{ts} > UAS-Rab7^{DN}*, Rab7^{DN} reroutes all traffic to clear vacuoles, thereby blocking access to the lysosome [Fu et al., 2017]) led to cytoplasmic accumulation of endocytosed PGN relative

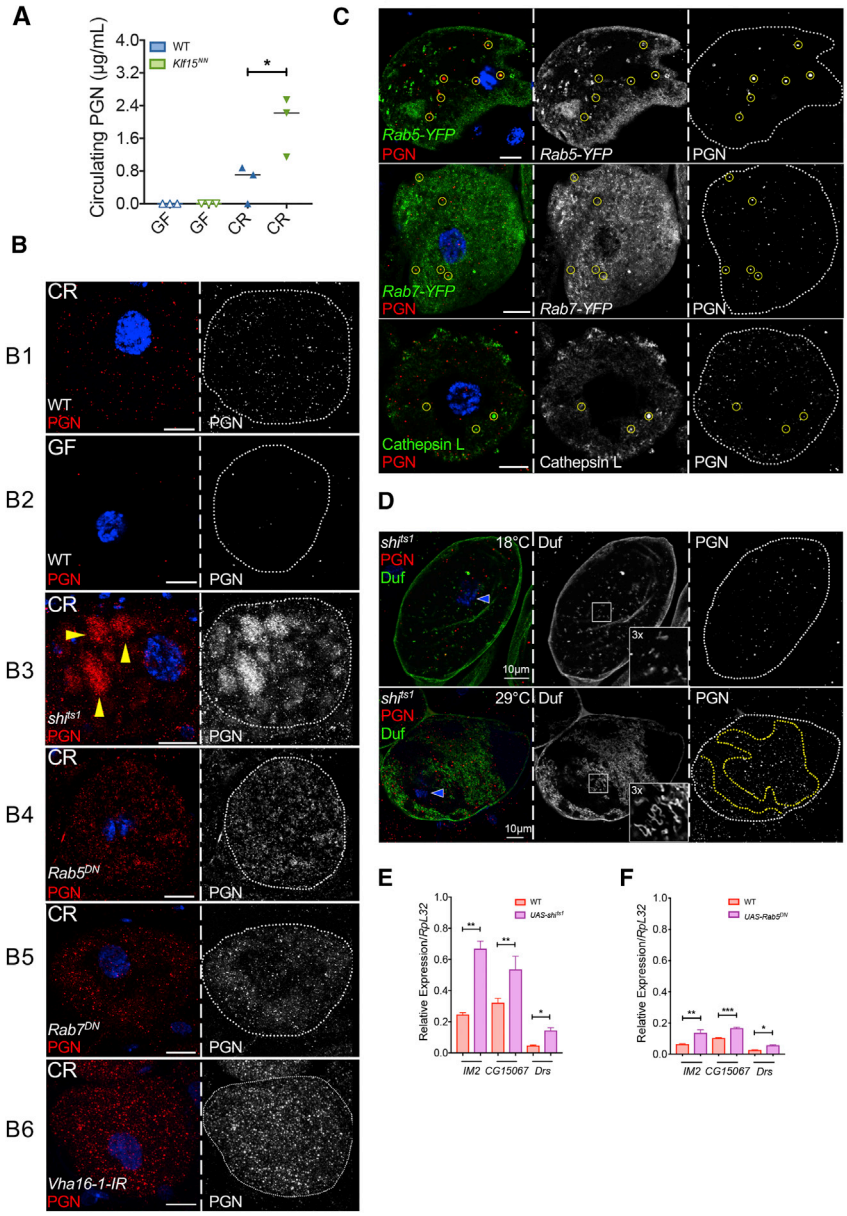

Figure 5. Nephrocytes Endocytose PGN from Systemic Circulation

(A) Quantification of PGN quantity in the hemolymph of WT and *Klf15*^{NN} flies in GF and CR conditions. *p < 0.05 in a Student's t test.

(B1 and B2) Immunostaining of nephrocytes from CR and GF flies with PGN antibody demonstrates that nephrocytes internalize microbiota-derived PGN.

(B3–B6) Nephrocyte-specific expression of *shibire*^{ts1} (*Dot-Gal4* > *UAS-shi*^{ts1}), *Rab5*^{DN} (*Hand-Gal4*^{ts} > *UAS-Rab5*^{DN}), *Rab7*^{DN} (*Hand-Gal4*^{ts} > *UAS-Rab7*^{DN}), and *Vha16-1-IR* (*Dot-Gal4* > *UAS-Vha16-1-IR*) led to accumulation of PGN in nephrocytes when compared to control (see Figure 5B1, 5D, S5D1 and S5D2 for additional controls). Scale bar, 10µm.

(C) Immunostaining against PGN reveals colocalization (yellow circles) with the early endosomal marker Rab5 (*Hand-Gal4*^{ts} > *UAS- Rab5-YFP*), the late endosomal marker Rab7 (*Hand-Gal4*^{ts} > *UAS-Rab7-YFP*), and the lysosomal compartment marker Cathepsin L. Scale bar, 10µm.

(D) Cortico-cytoplasmic view of nephrocytes immunostained with Duf (labels the lacunae) shows expansion of the lacunae (marked by the yellow dotted lines) in *shibire*^{ts1} (*Dot-Gal4* > *UAS-shi*^{ts1}) flies. Immunostaining with PGN antibody reveals that PGN is accumulating in the lacunae. Blue arrowheads are labeling the nuclei.

(E and F) Whole-fly qRT-PCR of Toll target genes *IM2*, *CG15067*, and *Drs* in unchallenged conditions. Gene expression was measured in flies expressing *shibire*^{ts1} and *Rab5*^{DN} in a nephrocyte-specific manner (*Dot-Gal4* > *UAS-shi*^{ts1} and *Hand-Gal4*^{ts} > *UAS-Rab5*^{DN}). *p < 0.05 **p < 0.01 ***p < 0.001 in a Student's t test.

to controls (Figures 5B4, 5B5, and S5D2, quantification in S5A). Since our data indicated that PGN is routed to the lysosomal compartment inside nephrocytes, we next assessed whether acidification of the lysosome is important for PGN degradation. Using *in vivo* RNAi, we decreased nephrocyte-specific expression of two key components of the vacuolar proton pump V-ATPase (*Dot-Gal4* > *UAS-Vha16-1-IR* and *Dot-Gal4* > *UAS-Vha44-IR*), which functions to acidify the endolysososmal compartment (Mauvezin et al., 2015). Blocking acidification of the endolysososmal compartment led to substantial PGN accumulation (Figures 5B6 and S5D3, quantification in S5A). Taken together, these results demonstrate that PGN is endocytosed and degraded by nephrocytes in a Shibire-, Rab5-, Rab7-, and V-ATPase-dependent manner.

Finally, we examined the consequences of arresting the endocytic function of nephrocytes on Toll pathway activity. Blocking endocytosis in nephrocytes via expression of the same *shibire*^{ts1} and *Rab5*^{DN} alleles was sufficient to induce abnormally high transcription of Toll target genes (Figures 5E and 5F). These results are in agreement with the increase in Toll pathway signaling we detected in flies in which *Klf15* expression was decreased by *in vivo* RNAi in adult nephrocytes (Figure 2F), a condition known to block their endocytic capability (Ivy et al., 2015). Altogether, our results establish that nephrocytes remove microbiota-derived PGN from systemic circulation, thus preventing deviant immune activation in response to gut microbes.

DISCUSSION

Toll and Imd, the two primary immune recognition pathways in the fly, detect the presence of invading bacteria through sensing of specific forms of PGN: the Toll pathway recognizes Lys-type PGN from Gram-positive bacteria, while the Imd pathway detects DAP-type PGN from Gram-negative bacteria and certain Gram-positive bacilli (Lemaitre and Hoffmann, 2007). Because the gut is constantly exposed to microbes and their PAMPs, it relies on specialized mechanisms to prevent local immune activation against the microbiota. Given

that microbiota-shed PGN translocates from the gut lumen into general circulation (Capo et al., 2017; Clarke et al., 2010; Corbitt et al., 2013; Gendrin et al., 2009; Paredes et al., 2011; Zaidman-Rémy et al., 2006), mechanisms are required to prevent systemic immune activation in response to these microbiota products. Without such processes, chronic immune induction can lead to abnormal development (Bischoff et al., 2006) and/or a shortened lifespan, indicating that uncontrolled immune activity can be costly to the host's health (Charroux et al., 2018; Guillou et al., 2016; Paredes et al., 2011). Mechanisms that prevent the systemic activation of Imd in response to the microbiota include the secretion of amidase PGRPs into the hemolymph, which act to degrade DAP-type PGN (Bischoff et al., 2006; Charroux et al., 2018; Guo et al., 2014; Paredes et al., 2011; Zaidman-Rémy et al., 2006). Here, we found that filtration of hemolymph by nephrocytes prevents chronic activation of the Toll pathway. Mechanistically, nephrocytes endocytose Lys-type PGN from systemic circulation and route it to lysosomes for degradation, thus maintaining immune homeostasis.

Why would an organism evolve distinct mechanisms to eliminate 2 types of PGN? One possibility is that efficient degradation of Lys-type PGN requires specialized enzymes, such as lysozymes, that work best in the acidified environment of a mature lysosome than in circulation. The optimal pH for *Drosophila* lysozyme activity is ~5 (Regel et al., 1998). By contrast, hemolymph pH is considerably higher, with pH values ranging from 7.3 to 7.4 (Ghosh and O'Connor, 2014). As nephrocytes are professional endocytic cells, they are well suited to rapidly and proficiently uptake Lys-type PGN from the hemolymph and route it for degradation to lysosomes. In support of this idea, it is worth noting that nephrocytes express at least 6 lysozyme-like genes (Chintapalli et al., 2007). Due to redundancy and a lack of genetic tools for all 6 lysozyme genes, we were not able to functionally test the role of these lysozymes in the degradation of PGN. Therefore, a role for lysozyme remains speculative. Interestingly, our data also established that the Imd pathway is not activated in the absence of nephrocytes. This may be a result of the efficient degradation of DAP-type PGN by amidase PGRPs, such that there is no remaining intact PGN of this class that needs to be filtered and endocytosed. Alternatively, the intrinsic negative charge of the nephrocyte basement membrane, which is known to act as a charge-selective filter (Denholm and Skaer, 2009), may act to exclude passage of DAP-type but not Lys-type PGN.

Nephrocytes uptake Nec, a secreted serpin and negative regulator of the Toll pathway, and target it for lysosomal degradation (Soukup et al., 2009). Our work not only confirmed this finding, as Nec protein concentration was higher in the hemolymph of $Klf15^{NN}$ flies compared to WT, but also found that other signaling components of the Toll pathway, such as SPE, accumulated in the hemolymph of $Klf15^{NN}$ flies in the absence of transcriptional changes. These results suggest that hemolymph filtration by nephrocytes may serve to regulate Toll pathway homeostasis on multiple levels—regulating the concentration of both Lys-type PGN and Toll pathway components in the hemolymph. We were unable to determine whether the accumulation of signaling components of the Toll pathway was also important for the loss of immune homeostasis in flies lacking nephrocytes. However, the fact that GF $Klf15^{NN}$ flies did not show an increase in Toll activity suggests that PGN filtration, rather than accumulation of Toll pathway signaling components, is the critical mechanism at work. In addition, we note that the phenotype associated with a lack of nephrocytes is not easily predicted. At first glance, accumulation of Nec in flies devoid of nephrocytes would suggest a possible decrease in immune reactivity. However, we found that the loss of PGN filtration primes the immune system and increases resistance to infection.

Chronic kidney disease (CKD), characterized by a gradual loss of glomerular filtration rate, leads to alterations in plasma protein content similar to those observed in $Klf15^{NN}$ flies. Specifically, proteomic analyses show that patients with CKD progressively accumulate in their plasma high quantities of 24 proteins involved in the complement system, as well as 62 proteins associated with the acute phase response (Glorieux et al., 2015). Given the remarkable functional, structural, and molecular similarities between nephrocytes and the glomerular podocytes of the mammalian kidney, we propose that renal filtration by the kidneys could also act to regulate the amount of microbiota-derived PAMPs, such as PGN, in the blood, thus maintaining immune homeostasis. In support of this idea, we highlight that the alternative complement pathway, several components of which are enriched in the plasma of CKD patients, is activated by PGN, including Lys-type PGN (Kawasaki et al., 1987). In both $Klf15^{NN}$ flies and CKD patients, proteomic studies also showed accumulation of lysozymes in circulation, with lysozyme C increasing in the plasma and the lysozyme encoded by *CG6426* rising in hemolymph. It is possible that lysozyme accumulation may result, in both cases, from induction of the immune system in response to PGN, especially as *CG6426* is a target of the Toll pathway (De Gregorio et al., 2001; Troha et al., 2018). Finally, it has been proposed that nephrocytes are functionally analogous to endocytic scavenger cells of the mammalian reticuloendothelial system (Sørensen et al., 2012; Wigglesworth, 1970). Therefore, it is possible that additional cells with scavenging function, such as hepatocytes, may also be involved in the regulation of circulating microbiota-shed PAMPs.

Altogether, our results reveal a role for podocyte filtration in the maintenance of insect immune homeostasis. The results suggest that renal clearance may be a major and conserved mechanism to remove PGN from circulation, thus preventing aberrant immune activation in response to the gut microbiota. Because of the parallels between the filtration systems of flies and mammals, as well as the similar consequences of altering renal function in both species, we propose that at least part of the immune activation observed in patients suffering from glomerular diseases may stem from the accumulation of PGN in plasma.

STAR★METHODS

Detailed methods are provided in the online version of this paper and include the following:

- KEY RESOURCES TABLE
- CONTACT FOR REAGENT AND RESOURCE SHARING
- EXPERIMENTAL MODEL AND SUBJECT DETAILS
  - Rearing of *Drosophila melanogaster*
  - *Drosophila melanogaster* strains
  - Culturing of microbes

SUPPLEMENTAL INFORMATION

Supplemental Information can be found online at https://doi.org/10.1016/j.immuni.2019.08.020.

ACKNOWLEDGMENTS

We thank J. Rossi for assistance with manuscript editing. We also thank all members of the Buchon lab for helpful comments on the manuscript. Finally, we thank Gábor Juhász for providing the *dLamp-3xmCherry* transgenic flies. The graphical abstract was created with BioRender. This work was supported by NSF IOS1656118 and NSF IOS1653021 to N.B.

AUTHOR CONTRIBUTIONS

Conceptualization, N.B., B.P.L., P.S.H., and K.T.; Data Curation, K.T., P.N., and A.P.; Formal Analysis, K.T. and P.N.; Methodology, K.T. and P.N.; Supervision, N.B. and B.P.L.; Validation, K.T. and P.N.; Visualization, K.T., P.S.H., and P.N.; Writing – Original Draft, K.T. and N.B.; Writing – Review & Editing, N.B., K.T., P.N., A.P., B.P.L., and P.S.H.

DECLARATION OF INTERESTS

The authors declare no competing interests.

Received: October 17, 2018
Revised: May 14, 2019
Accepted: August 27, 2019
Published: September 26, 2019

REFERENCES

Aggarwal, S.K., and King, R.C. (1967). The ultrastructure of the wreath cells of Drosophila melanogaster larvae. Protoplasma *63*, 343–352.

Aggarwal, K., Rus, F., Vriesema-Magnuson, C., Ertürk-Hasdemir, D., Paquette, N., and Silverman, N. (2008). Rudra interrupts receptor signaling complexes to negatively regulate the IMD pathway. PLoS Pathog. *4*, e1000120.

Ayres, J.S., and Schneider, D.S. (2012). Tolerance of Infections. Annu. Rev. Immunol. *30*, 271–294.

Basbous, N., Coste, F., Leone, P., Vincentelli, R., Royet, J., Kellenberger, C., and Roussel, A. (2011). The Drosophila peptidoglycan-recognition protein LF interacts with peptidoglycan-recognition protein LC to downregulate the Imd pathway. EMBO Rep. *12*, 327–333.

Binggeli, O., Neyen, C., Poidevin, M., and Lemaitre, B. (2014). Prophenoloxidase activation is required for survival to microbial infections in Drosophila. PLoS Pathog. *10*, e1004067.

Bischoff, V., Vignal, C., Duvic, B., Boneca, I.G., Hoffmann, J.A., and Royet, J. (2006). Downregulation of the Drosophila immune response by peptidoglycan-recognition proteins SC1 and SC2. PLoS Pathog. *2*, e14.

Bischoff, V., Vignal, C., Boneca, I.G., Michel, T., Hoffmann, J.A., and Royet, J. (2004). Function of the drosophila pattern-recognition receptor PGRP-SD in the detection of Gram-positive bacteria. Nature Immunology *5*, 1175–1180.

Broderick, N.A., Buchon, N., and Lemaitre, B. (2014). Microbiota-induced changes in drosophila melanogaster host gene expression and gut morphology. MBio *5*, e01117–e14.

Buchon, N., Poidevin, M., Kwon, H.-M., Guillou, A., Sottas, V., Lee, B.L., and Lemaitre, B. (2009). A single modular serine protease integrates signals from pattern-recognition receptors upstream of the Drosophila Toll pathway. Proc. Natl. Acad. Sci. USA *106*, 12442–12447.

Buchon, N., Silverman, N., and Cherry, S. (2014). Immunity in Drosophila melanogaster–from microbial recognition to whole-organism physiology. Nat. Rev. Immunol. *14*, 796–810.

Cao, Y., Chtarbanova, S., Petersen, A.J., and Ganetzky, B. (2013). Dnr1 mutations cause neurodegeneration in Drosophila by activating the innate immune response in the brain. Proc. Natl. Acad. Sci. USA *110*, E1752–E1760.

Capo, F., Chaduli, D., Viallat-Lieutaud, A., Charroux, B., and Royet, J. (2017). Oligopeptide Transporters of the SLC15 Family Are Dispensable for Peptidoglycan Sensing and Transport in Drosophila. J. Innate Immun. *9*, 483–492.

Cecconi, M., Evans, L., Levy, M., and Rhodes, A. (2018). Sepsis and septic shock. Lancet *392*, 75–87.

Charroux, B., Capo, F., Kurz, C.L., Peslier, S., Chaduli, D., Viallat-Lieutaud, A., and Royet, J. (2018). Cytosolic and Secreted Peptidoglycan-Degrading Enzymes in Drosophila Respectively Control Local and Systemic Immune Responses to Microbiota. Cell Host Microbe *23*, 215–228.e4.

Chintapalli, V.R., Wang, J., and Dow, J.A.T. (2007). Using FlyAtlas to identify better Drosophila melanogaster models of human disease. Nat. Genet. *39*, 715–720.

Clarke, T.B., Davis, K.M., Lysenko, E.S., Zhou, A.Y., Yu, Y., and Weiser, J.N. (2010). Recognition of peptidoglycan from the microbiota by Nod1 enhances systemic innate immunity. Nat. Med. *16*, 228–231.

Corbitt, N., Kimura, S., Isse, K., Specht, S., Chedwick, L., Rosborough, B.R., Lunz, J.G., Murase, N., Yokota, S., and Demetris, A.J. (2013). Gut bacteria drive Kupffer cell expansion via MAMP-mediated ICAM-1 induction on sinusoidal endothelium and influence preservation-reperfusion injury after orthotopic liver transplantation. Am. J. Pathol. *182*, 180–191.

Crossley, A.C. (1972). The ultrastructure and function of pericardial cells and other nephrocytes in an insect: Calliphora erythrocephala. Tissue Cell *4*, 529–560.

De Gregorio, E., Han, S.-J., Lee, W.-J., Baek, M.-J., Osaki, T., Kawabata, S., Lee, B.-L., Iwanaga, S., Lemaitre, B., and Brey, P.T. (2002). An immune-responsive Serpin regulates the melanization cascade in Drosophila. Dev. Cell *3*, 581–592.

De Gregorio, E., Spellman, P.T., Rubin, G.M., and Lemaitre, B. (2001). Genome-wide analysis of the Drosophila immune response by using oligonucleotide microarrays. Proc. Natl. Acad. Sci. U S A. *98*, 12590–12595.

Denholm, B., and Skaer, H. (2009). Bringing together components of the fly renal system. Curr. Opin. Genet. Dev. *19*, 526–532.

Dudzic, J.P., Kondo, S., Ueda, R., Bergman, C.M., and Lemaitre, B. (2015). Drosophila innate immunity: regional and functional specialization of prophenoloxidases. BMC Biol. *13*, 81.

Duneau, D., Ferdy, J.-B., Revah, J., Kondolf, H., Ortiz, G.A., Lazzaro, B.P., and Buchon, N. (2017). Stochastic variation in the initial phase of bacterial infection predicts the probability of survival in D. melanogaster. elife *6*, e28298.

Elrod-Erickson, M., Mishra, S., and Schneider, D.S. (2000). Interactions between the cellular and humoral immune responses in Drosophila 10, pp. 781–784.

Fu, Y., Zhu, J.-Y., Zhang, F., Richman, A., Zhao, Z., and Han, Z. (2017). Comprehensive functional analysis of Rab GTPases in Drosophila nephrocytes. Cell Tissue Res. *368*, 615–627.

Gendrin, M., Welchman, D.P., Poidevin, M., Hervé, M., and Lemaitre, B. (2009). Long-range activation of systemic immunity through peptidoglycan diffusion in Drosophila. PLoS Pathog. *5*, e1000694.

Ghosh, A.C., and O'Connor, M.B. (2014). Systemic Activin signaling independently regulates sugar homeostasis, cellular metabolism, and pH balance in Drosophila melanogaster. Proc. Natl. Acad. Sci. USA *111*, 5729–5734.

Glorieux, G., Mullen, W., Duranton, F., Filip, S., Gayrard, N., Husi, H., Schepers, E., Neirynck, N., Schanstra, J.P., Jankowski, J., et al. (2015). New insights in molecular mechanisms involved in chronic kidney disease using high-resolution plasma proteome analysis. Nephrol. Dial. Transplant. *30*, 1842–1852.

Gobert, V. (2003). Dual Activation of the Drosophila Toll Pathway by Two Pattern Recognition Receptors. Science *302*, 2126–2130.

Gordon, M.D., Ayres, J.S., Schneider, D.S., and Nusse, R. (2008). Pathogenesis of listeria-infected Drosophila wntD mutants is associated with elevated levels of the novel immunity gene edin. PLoS Pathog. *4*, e1000111.

Gottar, M., Gobert, V., Matskevich, A.A., Reichhart, J.M., Wang, C., Butt, T.M., Belvin, M., Hoffmann, J.A., and Ferrandon, D. (2006). Dual detection of fungal infections in Drosophila via recognition of glucans and sensing of virulence factors. Cell *127*, 1425–1437.

Guillou, A., Troha, K., Wang, H., Franc, N.C., and Buchon, N. (2016). The Drosophila CD36 Homologue croquemort Is Required to Maintain Immune and Gut Homeostasis during Development and Aging. PLoS Pathog. *12*, e1005961.

Guo, L., Karpac, J., Tran, S.L., and Jasper, H. (2014). PGRP-SC2 promotes gut immune homeostasis to limit commensal dysbiosis and extend lifespan. Cell *156*, 109–122.

Hartley, P.S., Motamedchaboki, K., Bodmer, R., and Ocorr, K. (2016). SPARC-Dependent Cardiomyopathy in Drosophila. Circ Cardiovasc Genet *9*, 119–129.

Hegedűs, K., Takáts, S., Boda, A., Jipa, A., Nagy, P., Varga, K., Kovács, A.L., and Juhász, G. (2016). The Ccz1-Mon1-Rab7 module and Rab5 control distinct steps of autophagy. Mol. Biol. Cell *27*, 3132–3142.

Ivy, J.R., Drechsler, M., Catterson, J.H., Bodmer, R., Ocorr, K., Paululat, A., and Hartley, P.S. (2015). Klf15 Is Critical for the Development and Differentiation of Drosophila Nephrocytes. PLoS ONE *10*, e0134620.

Jang, I.-H., Chosa, N., Kim, S.-H., Nam, H.-J., Lemaitre, B., Ochiai, M., Kambris, Z., Brun, S., Hashimoto, C., Ashida, M., et al. (2006). A Spätzle-processing enzyme required for toll signaling activation in Drosophila innate immunity. Dev. Cell *10*, 45–55.

Kaneko, T., Goldman, W.E., Mellroth, P., Steiner, H., Fukase, K., Kusumoto, S., Harley, W., Fox, A., Golenbock, D., and Silverman, N. (2004). Monomeric and polymeric gram-negative peptidoglycan but not purified LPS stimulate the Drosophila IMD pathway. Immunity *20*, 637–649.

Kaneko, T., Yano, T., Aggarwal, K., Lim, J.-H., Ueda, K., Oshima, Y., Peach, C., Erturk-Hasdemir, D., Goldman, W.E., Oh, B.-H., et al. (2006). PGRP-LC and PGRP-LE have essential yet distinct functions in the drosophila immune response to monomeric DAP-type peptidoglycan. Nat. Immunol. *7*, 715–723.

Kawasaki, A., Takada, H., Kotani, S., Inai, S., Nagaki, K., Matsumoto, M., Yokogawa, K., Kawata, S., Kusumoto, S., and Shiba, T. (1987). Activation of the human complement cascade by bacterial cell walls, peptidoglycans, water-soluble peptidoglycan components, and synthetic muramylpeptides–studies on active components and structural requirements. Microbiol. Immunol. *31*, 551–569.

Kleino, A., Myllymäki, H., Kallio, J., Vanha-aho, L.-M., Oksanen, K., Ulvila, J., Hultmark, D., Valanne, S., and Rämet, M. (2008). Pirk is a negative regulator of the Drosophila Imd pathway. J. Immunol. *180*, 5413–5422.

Kosaka, T., and Ikeda, K. (1983). Reversible blockage of membrane retrieval and endocytosis in the garland cell of the temperature-sensitive mutant of Drosophila melanogaster, shibirets1. J. Cell Biol. *97*, 499–507.

Lemaitre, B., and Hoffmann, J. (2007). The host defense of Drosophila melanogaster. Annu. Rev. Immunol. *25*, 697–743.

Levashina, E.A., Langley, E., Green, C., Gubb, D., Ashburner, M., Hoffmann, J.A., and Reichhart, J.M. (1999). Constitutive activation of toll-mediated antifungal defense in serpin-deficient Drosophila. Science *285*, 1917–1919.

Lhocine, N., Ribeiro, P.S., Buchon, N., Wepf, A., Wilson, R., Tenev, T., Lemaitre, B., Gstaiger, M., Meier, P., and Leulier, F. (2008). PIMS modulates immune tolerance by negatively regulating Drosophila innate immune signaling. Cell Host Microbe *4*, 147–158.

Liu, X., Hodgson, J.J., and Buchon, N. (2017). Drosophila as a model for homeostatic, antibacterial, and antiviral mechanisms in the gut. PLoS Pathog. *13*, e1006277.

Maillet, F., Bischoff, V., Vignal, C., Hoffmann, J., and Royet, J. (2008). The Drosophila peptidoglycan recognition protein PGRP-LF blocks PGRP-LC and IMD/JNK pathway activation. Cell Host Microbe *3*, 293–303.

Mallipattu, S.K., Liu, R., Zheng, F., Narla, G., Ma'ayan, A., Dikman, S., Jain, M.K., Saleem, M., D'Agati, V., Klotman, P., et al. (2012). Kruppel-like factor 15 (KLF15) is a key regulator of podocyte differentiation. J. Biol. Chem. *287*, 19122–19135.

Mauvezin, C., Nagy, P., Juhász, G., and Neufeld, T.P. (2015). Autophagosome-lysosome fusion is independent of V-ATPase-mediated acidification. Nat. Commun. *6*, 7007.

Michel, T., Reichhart, J.M., Hoffmann, J.A., and Royet, J. (2001). Drosophila Toll is activated by Gram-positive bacteria through a circulating peptidoglycan recognition protein. Nature *414*, 756–759.

Ming, M., Obata, F., Kuranaga, E., and Miura, M. (2014). Persephone/Spätzle pathogen sensors mediate the activation of Toll receptor signaling in response to endogenous danger signals in apoptosis-deficient Drosophila. J. Biol. Chem. *289*, 7558–7568.

Na, J., and Cagan, R. (2013). The Drosophila nephrocyte: back on stage. J. Am. Soc. Nephrol. *24*, 161–163.

Newton, K., and Dixit, V.M. (2012). Signaling in innate immunity and inflammation. Cold Spring Harb. Perspect. Biol. *4*, a006049–a006049.

Paredes, J.C., Welchman, D.P., Poidevin, M., and Lemaitre, B. (2011). Negative regulation by amidase PGRPs shapes the Drosophila antibacterial response and protects the fly from innocuous infection. Immunity *35*, 770–779.

Park, J.-W., Kim, C.-H., Kim, J.-H., Je, B.-R., Roh, K.-B., Kim, S.-J., Lee, H.-H., Ryu, J.-H., Lim, J.-H., Oh, B.-H., Lee, W.-J., Ha, N.-C., Lee, B.-L., et al. (2007). Clustering of peptidoglycan recognition protein-SA is required for sensing lysine-type peptidoglycan in insects. Proc. Natl. Acad. Sci. U S A. *104*, 6602–6607.

Psathaki, O.-E., Dehnen, L., Hartley, P.S., and Paululat, A. (2018). Drosophila pericardial nephrocyte ultrastructure changes during ageing. Mech. Ageing Dev. *173*, 9–20.

Regel, R., Matioli, S.R., and Terra, W.R. (1998). Molecular adaptation of Drosophila melanogaster lysozymes to a digestive function. Insect Biochem. Mol. Biol. *28*, 309–319.

Reiser, J., and Altintas, M.M. (2016). Podocytes. F1000Res. *5*. F1000 Faculty Rev-114. https://doi.org/10.12688/f1000research.7255.1.

Ryu, J.-H., Kim, S.-H., Lee, H.-Y., Bai, J.Y., Nam, Y.-D., Bae, J.-W., Lee, D.G., Shin, S.C., Ha, E.-M., and Lee, W.-J. (2008). Innate immune homeostasis by the homeobox gene caudal and commensal-gut mutualism in Drosophila. Science *319*, 777–782.

Salvetti, E., Torriani, S., and Felis, G.E. (2012). The Genus Lactobacillus: A Taxonomic Update. Probiotics Antimicrob. Proteins *4*, 217–226.

Scherfer, C., Tang, H., Kambris, Z., Lhocine, N., Hashimoto, C., and Lemaitre, B. (2008). Drosophila Serpin-28D regulates hemolymph phenoloxidase activity and adult pigmentation. Dev. Biol. *323*, 189–196.

Schleifer, K.H., and Kandler, O. (1972). Peptidoglycan types of bacterial cell walls and their taxonomic implications. Bacteriol. Rev. *36*, 407–477.

Sørensen, K.K., McCourt, P., Berg, T., Crossley, C., Le Couteur, D., Wake, K., and Smedsrød, B. (2012). The scavenger endothelial cell: a new player in homeostasis and immunity. Am. J. Physiol. Regul. Integr. Comp. Physiol. *303*, R1217–R1230.

Soukup, S.F., Culi, J., and Gubb, D. (2009). Uptake of the necrotic serpin in Drosophila melanogaster via the lipophorin receptor-1. PLoS Genet. *5*, e1000532.

Thevenon, D., Engel, E., Avet-Rochex, A., Gottar, M., Bergeret, E., Tricoire, H., Benaud, C., Baudier, J., Taillebourg, E., and Fauvarque, M.-O. (2009). The Drosophila ubiquitin-specific protease dUSP36/Scny targets IMD to prevent constitutive immune signaling. Cell Host Microbe *6*, 309–320.

Troha, K., and Buchon, N. (2019). Methods for the study of innate immunity in Drosophila melanogaster. Wiley Interdiscip. Rev. Dev. Biol. *8*, e344.

Troha, K., Im, J.H., Revah, J., Lazzaro, B.P., and Buchon, N. (2018). Comparative transcriptomics reveals CrebA as a novel regulator of infection tolerance in D. melanogaster. PLoS Pathog. *14*, e1006847.

Weavers, H., Prieto-Sánchez, S., Grawe, F., Garcia-López, A., Artero, R., Wilsch-Bräuninger, M., Ruiz-Gómez, M., Skaer, H., and Denholm, B. (2009). The insect nephrocyte is a podocyte-like cell with a filtration slit diaphragm. Nature *457*, 322–326.

Wigglesworth, V.B. (1970). The pericardial cells of insects: analogue of the reticuloendothelial system. J. Reticuloendothel. Soc. *7*, 208–216.

Zaidman-Rémy, A., Hervé, M., Poidevin, M., Pili-Floury, S., Kim, M.-S., Blanot, D., Oh, B.-H., Ueda, R., Mengin-Lecreulx, D., and Lemaitre, B. (2006). The Drosophila amidase PGRP-LB modulates the immune response to bacterial infection. Immunity *24*, 463–473.

Zhang, F., Zhao, Y., and Han, Z. (2013). An in vivo functional analysis system for renal gene discovery in Drosophila pericardial nephrocytes. J. Am. Soc. Nephrol. *24*, 191–197.

Zhuang, S., Shao, H., Guo, F., Trimble, R., Pearce, E., and Abmayr, S.M. (2009). Sns and Kirre, the Drosophila orthologs of Nephrin and Neph1, direct adhesion, fusion and formation of a slit diaphragm-like structure in insect nephrocytes. Development *136*, 2335–2344.

STAR★METHODS

KEY RESOURCES TABLE

REAGENT or RESOURCE	SOURCE	IDENTIFIER
Antibodies		
Anti-Peptidoglycan Antibody (mouse monoclonal)	GeneTex	Cat#GTX39437; RRID:AB_11173396
Bacterial and Virus Strains		
Enterococcus faecalis	This strain is available upon request (see Troha et al., 2018).	RRID:N/A
Staphylococcus aureus	This strain is available upon request (see Troha et al., 2018).	RRID:N/A
Critical Commercial Assays		
SLP (Silkworm Larvae Plasma) Reagent Set	Fujifilm Wako Pure Chemical Corporation	Cat#297-51501; RRID:N/A
Deposited Data		
Proteomic Analysis of Hemolymph Proteome (Dataset)	See Hartley et al., 2016	RRID:N/A
Experimental Models: Organisms/Strains		
Drosophila: WT: w^{1118}	This strain is available upon request (see Ivy et al., 2015).	RRID:N/A
Drosophila: *Klf15*: $Klf15^{NN}$	This strain is available upon request (see Ivy et al., 2015).	RRID:N/A
Drosophila: *UAS-shi*^{ts1}: *UAS-shi*^{ts1}	Bloomington *Drosophila* Stock Center	Cat#44222; RRID:BDSC_44222
Drosophila: *Dot-Gal4*: *Dot-Gal4*	This strain is available upon request (see Ivy et al., 2015).	RRID:N/A
Drosophila: *Hand-Gal4*^{ts}: *Hand-Gal4*^{ts}	This strain is available upon request (see Ivy et al., 2015).	RRID:N/A
Oligonucleotides		
Gene: IM2 Forward Primer (5′ to 3′) ACCGTCTTTGTGTTCGGTCT Reverse Primer (5′ to 3′) TGCAGTCCCCGTTGATTACC	FlyPrimerBank	Cat#PD40206; RRID:N/A
Gene: CG15067 Forward Primer (5′ to 3′) GAGCCTGACGTTATTGGCG Reverse Primer (5′ to 3′) CCTTTTCCACTTGTTGGCTTGT	FlyPrimerBank	Cat#PP1866; RRID:N/A

CONTACT FOR REAGENT AND RESOURCE SHARING

Further information and requests for resources and reagents should be directed to and will be fulfilled by the Lead Contact, Nicolas Buchon (nicolas.buchon@cornell.edu).

This study did not generate new unique reagents.

EXPERIMENTAL MODEL AND SUBJECT DETAILS

Rearing of *Drosophila melanogaster*

Flies were maintained on standard sucrose-cornmeal-yeast medium: 50 g baker's yeast, 60 g cornmeal, 40 g sucrose, 7 g agar, 26.5 mL Moldex (10%), and 12 mL Acid Mix solution (4.2% phosphoric acid, 41.8% propionic acid) per 1L of deionized H_2O. Wild-type and mutant flies were raised at 24°C. Flies originating from crosses that employ the UAS-Gal4-Gal80^{ts} gene expression system were raised at 18°C (Gal80^{ts} On, Gal4 Off) and transferred to 29°C (Gal80^{ts} Off, Gal4 On) 5 days after eclosion. Males were used for all experiments, with the exception of immunostaining (larger female size is preferred for dissection and visualization of cells). For experiments with mutants, 5- to 8-day-old adult flies were used. For experiments with *UAS* transgenes, 10- to 14-day-old flies were used (to allow for the expression of the pertinent construct).

Drosophila melanogaster strains

Klf15^{NN}, *spz*^{rm7}, *SPE*^{SK6}, *psh*^{1}, *modSP*^{1}, *GNBP3*^{Hades}, *PGRP-SA*^{seml}, and *PPO1*$^{\Delta}$, *2*$^{\Delta}$,*3*^{1} mutants and the *dLamp-3xmCherry* lysosomal marker have been previously described (Buchon et al., 2009; Dudzic et al., 2015; Gobert, 2003; Gottar et al., 2006; Hegedűs et al., 2016; Ivy et al., 2015; Jang et al., 2006; Michel et al., 2001; Ming et al., 2014). The nephrocyte-specific drivers, *Dot-Gal4* and *Hand-Gal4*^{ts}, are detailed in (Ivy et al., 2015). The following lines were purchased from the Bloomington *Drosophila* Stock Center: *UAS-shi*^{ts1} (44222), *UAS-Rab5*^{DN} (9771), *UAS-Rab7*^{DN} (9778), *UAS-Rab5-YFP* (24616), *UAS-Rab7-YFP* (23270). The following lines were purchased from the Vienna *Drosophila* Resource Center: *UAS-Vha16-IR* (49290) and *UAS-Vha44-IR* (46563).

Culturing of microbes

The following bacteria were cultured overnight in LB broth and adjusted to the specified density: *Serratia marcescens* Type (OD_{600} = 1), *Salmonella typhimurium* (OD_{600} = 1), *Listeria innocua* (OD_{600} = 1), *Enterococcus faecalis* (OD_{600} = 1), *Staphylococcus aureus* (OD_{600} = 1), and *Providencia rettgeri* (OD_{600} = 1). *S. typhimurium* and *L. innocua* were grown at 37°C. All other bacteria were grown at 29°C. The fungi *Beauveria bassiana* and *Metarhizium anisopliae* were grown at 29°C on YPG-agar plates.

METHOD DETAILS

Infection, survival, and lifespan experiments

Flies were systemically infected with bacteria via septic pinprick to the thorax. Pinprick infection with an OD_{600} = 1 for the bacteria aforementioned results in inoculation with ~3,000 CFU/fly. For natural infections with fungi, CO_2-anaestethized flies were placed directly on the sporulating lawn of a fungal culture plate and the plate was shaken for ~15 s to coat the flies in spores. Flies were then transferred to a new, clean food vial to recover. All flies, regardless of infection method, were maintained at 29°C for the duration of the experiments. For survival experiments, death was recorded daily following inoculation, with flies transferred to fresh vials every 2 to 3 days. For lifespan measurements, adults were transferred to 29°C 5 days post-eclosion and remained at that temperature for the duration of the experiment. All experiments were performed at least 3 times.

Quantification of bacterial CFUs

At specified time points following inoculation, flies were individually homogenized by bead beating in 500 μl of sterile PBS using a tissue homogenizer (OPS Diagnostics). Dilutions of the homogenate were plated onto LB agar plates using a WASP II autoplate spiral plater (Microbiology International), incubated overnight at 29°C, and CFUs were counted. All experiments were performed at least 3 times.

RT-qPCR

For all experiments involving RT-qPCR, total RNA was extracted from pools of 20 flies using the standard TRIzol (Invitrogen) extraction. RNA samples were treated with DNase (Promega), and cDNA was generated using murine leukemia virus reverse transcriptase (MLV-RT-Promega). qPCR was performed using the SSO Advanced SYBR green kit (Bio-Rad) in a Bio-Rad CFX-Connect instrument. Data represent the relative ratio of the target gene and that of the reference gene *RpL32*. Mean values of at least three biological replicates are represented ± SE. The oligonucleotide sequences used can be found in Table S1.

Phagocytosis assays

To assay phagocytosis, flies were injected in the thorax with 69 nL of pHrodo Red Bioparticles (Invitrogen) using a Nanoject (Drummond Scientific). The fluorescence within the abdomen of the flies was then imaged at 3 h post-injection with a Leica MZFLIII fluorescent microscope and quantified using ImageJ (NIH) as previously described (Guillou et al., 2016). To block phagocytosis, adult flies were pre-injected with a solution containing latex beads as previously described in (Elrod-Erickson et al., 2000). Twenty-four h post injection, the flies were subjected to systemic infection as described above.

Hemolymph extraction

Hemolymph was collected using a centrifugation or capillary method. In the first method, ~100 anesthetized flies are loaded into a modified spin column (QIAGEN), in which the filter was removed and thoroughly washed with water before use, and 2 metal beads are placed on top of the flies. Flies are then centrifuged twice at 5,000 g for 5 min at 4°C. For more details, see (Troha and Buchon, 2019). For the capillary method, a pulled glass needle is used to prick flies in the thorax. Hemolymph is extracted into the needle by capillary action.

DOPA assay

Extracted hemolymph was immediately diluted in a 1:10 ratio using a protease inhibitor cocktail (Sigma: 11697498001) and kept on ice. Briefly, 50 μL of diluted hemolymph was combined with 150 μl of a 5 mM $CaCl_2$ solution and 800 μL of L-DOPA (Sigma: D9628) reagent. Following thorough mixing, 200 μl of sample/well was loaded into a 96-well plate. Using a spectrophotometer set to 29°C, a kinetic assay was performed at OD_{492}.

Generation of GF and mono-colonized flies

Collected eggs were surface sterilized by immersion in 70% ethanol for 2 min. Eggs were then dechorionated via treatment with a 10% bleach solution for 10 min. This was followed by rinsing the eggs in sterile water 3 times to remove any leftover bleach. The eggs were then transferred to pre-autoclaved media vials, where they were allowed to develop. The entire procedure was performed using sterile technique in a laminar flow hood. For mono-colonized flies, pre-autoclaved media vials were seeded with 200 μL of the desired individual bacterial culture (OD_{600} = 200). After the bacterial solution was absorbed into the media, adult germ-free flies were flipped into the mono-colonized media vial. Experiments with mono-colonized flies were carried out 5 days after the flies were first exposed to the bacteria.

PGN detection by SLP assay

The Silkworm Larvae Plasma (SLP) assay was used. After diluting extracted hemolymph (1:10 ratio), 50 μL of hemolymph sample/condition was used for the SLP assay (Fujifilm Wako Pure Chemical Corporation: 297-51501) following the manufacturer's instructions.

Gut barrier integrity (Smurf) assay

Adult flies were fed standard medium supplemented with Blue Dye No. 1 (2.5%). A fly was counted as a Smurf when the blue dye could be observed outside of the digestive tract.

UAS/GAL4/GAL80^{ts} gene expression system

For RNAi and overexpression experiments, we used the UAS/GAL4 gene expression system in combination with GAL80ts to restrict the expression of the constructs specifically to the adult stage. Flies were collected 5 to 8 days after eclosion from the pupal case and shifted to 29°C for an additional 8 days prior to any experiments. See our *Rearing of Drosophila melanogaster* section for additional details.

Immunohistochemistry and fluorescence imaging

Dissected nephrocytes were fixed in a 4% paraformaldehyde solution in PBST (PBS with 0.5% Triton X-100) for 1 h. After repeated washes in PBST, samples were blocked in 3% BSA PBST for 3 h and incubated overnight with primary antibodies in 1% BSA PBST at 4°C. Samples were labeled with secondary antibodies in 1% BSA PBST for 2 h. Samples were washed after each antibody labeling step with PBST containing 4% NaCl to reduce non-specific background labeling. The primary antibodies used in this study were: mouse anti-peptidoglycan (GeneTex: GTX39437) diluted 1:200, chicken anti-GFP (Invitrogen: A10262) diluted 1:1500, rabbit anti-Cathepsin L (Abcam: ab58991) diluted 1:1000, rabbit anti-Dumbfounded diluted 1:100 (Psathaki et al., 2018), and rabbit anti-RFP (Invitrogen: R10367) diluted 1:2000. The secondary antibodies were: Alexa Fluor 488 anti-chicken (A11039), Alexa Fluor 488 anti-rabbit (A21206), Alexa Fluor 488 anti-mouse (A21202), Alexa Fluor 555 anti-rabbit (A31572), and Alexa Fluor 555 anti-mouse (A31570), all diluted 1:1500 and from Invitrogen. Imaging was performed on a Zeiss LSM 700 confocal inverted microscope. Pearson correlation coefficients were calculated using ImageJ (FIJI, version: 2.0.0-rc-69/1.52n).

QUANTIFICATION AND STATISTICAL ANALYSIS

Aside from one exception, all analyses were performed in Prism (GraphPad Prism V7.0a, GraphPad Software, La Jolla, CA, USA). For survival assays, the curves represent the average percent survival ± SE of three or more biological replicates (n = 20 flies for each biological replicate). A Log-rank test was used to determine significance (*$p < 0.05$ **$p < 0.01$ ***$p < 0.001$ ****$p < 0.0001$). In bacterial load quantification assays, the horizontal lines represent median values for each time point. Three biological replicates were included. Following normalization, results were analyzed using a two-way ANOVA followed by Sidak's post-test for specific comparisons (*$p < 0.05$ **$p < 0.01$ ***$p < 0.001$ ****$p < 0.0001$). For all other experiments, mean values of three or more biological repeats are presented ± SE. Significance was calculated by a Student's t test following normalization (*$p < 0.05$ **$p < 0.01$ ***$p < 0.001$ ****$p < 0.0001$). Whenever survival curves crossed, a Cox's proportional-hazards model was used instead of a Log-rank test to assay significance. In this case, SPSS (IBM Corp. Released 2017. IBM SPSS Statistics for Mac OS X, Armonk, NY: IBM Corp.) was used for the analysis.

DATA AND CODE AVAILABILITY

This study did not generate datasets/code.